

Metal–Ligand Proton Tautomerism, Electron Transfer, and C(sp³)–H Activation by a 4-Pyridinyl-Pincer Iridium Hydride Complex

Tariq M. Bhatti, Akshai Kumar, Ashish Parihar, Hellan K. Moncy, Thomas J. Emge, Kate M. Waldie, Faraj Hasanayn,* and Alan S. Goldman*



Cite This: *J. Am. Chem. Soc.* 2023, 145, 18296–18306



Read Online

ACCESS |



Metrics & More

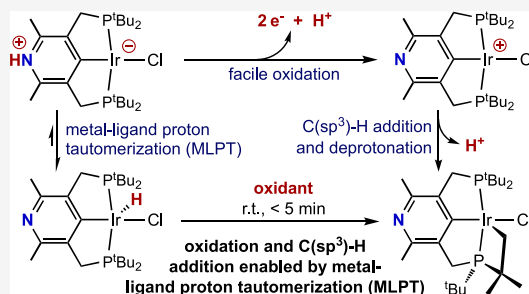


Article Recommendations



Supporting Information

ABSTRACT: The *para*-N-pyridyl-based PCP pincer proligand 3,5-bis(di-*tert*-butylphosphinomethyl)-2,6-dimethylpyridine (pN-^{tbu}PCP-H) was synthesized and metalated to give the iridium complex (pN-^{tbu}PCP)IrHCl (**2-H**). In marked contrast to its phenyl-based congeners, e.g., (^{tbu}PCP)IrHCl and derivatives, **2-H** is highly air-sensitive and reacts with oxidants such as ferrocenium, trityl cation, and benzoquinone. These oxidations ultimately lead to intramolecular activation of a phosphino-*t*-butyl C(sp³)–H bond and cyclometalation. Considering the greater electronegativity of N than C, **2-H** is expected to be less easily oxidized than simple PCP derivatives; cyclic voltammetry and DFT calculations support this expectation. However, **2-H** is calculated to undergo metal–ligand-proton tautomerism (MLPT) to give an N-protonated complex that can be described with resonance forms representing a zwitterionic complex (with a negative charge on Ir) and a *p*-N-pyridylidene (a remote N-heterocyclic carbene) Ir(I) complex. One-electron oxidation of this tautomer is calculated to be dramatically more favorable than direct oxidation of **2-H** ($\Delta\Delta G^\circ = -31.3$ kcal/mol). The resulting Ir(II) oxidation product is easily deprotonated to give metalloradical **2[•]** which is observed by NMR spectroscopy. **2[•]** can be further oxidized to give cationic Ir(III) complex, **2⁺**, which can oxidatively add a phosphino-*t*-butyl C–H bond and undergo deprotonation to give the observed cyclometalated product. DFT calculations indicate that less sterically hindered analogues of **2⁺** would preferentially undergo intermolecular addition of C(sp³)–H bonds, for example, of *n*-alkanes. The resulting iridium alkyl complexes could undergo facile β -H elimination to afford olefin, thereby completing a catalytic cycle for alkane dehydrogenation driven by one-electron oxidation and deprotonation, enabled by MLPT.



1. INTRODUCTION

Organometallic pyridinyl and pyridylidene ligands (Scheme 1) are a rich platform for multifunctional and noninnocent reactivity. Pincer ligands are privileged scaffolds in organometallic chemistry, with a wide variety of catalytic applications. Both emerged in the 1970s,^{1,2} and while neither took inspiration from nature at the time, the discovery of a pyridylidene-pincer nickel cofactor in lactate racemase is a gratifying example of their merger in recent years.^{3,4}

Pyridinyl and especially pyridylidene ligands can be viewed as a class of Fischer carbenes^{2,5–12} in which $p(\pi)$ electrons of the pyridyl nitrogen and the backbonding d -electrons of the metal compete to populate a vacant p orbital on the ipso carbon.¹³ The remote nitrogen therefore strongly influences the electronics at the metal center, enabling electronic switchability and proton-responsiveness.^{14,15} Quaternizing the nitrogen results in a significant increase of positive charge at the metal center, including examples with “P(C-pyridinyl)P”-pincer complexes.^{16,17} Milstein and co-workers have studied P(C-pyridinyl)P-pincer ruthenium complexes as platforms for metal–ligand cooperative aromatization/dearomatization, enabling diverse reactivity including dihydrogen activation, alcohol

dehydrogenation, and alcohol-amine dehydrogenative coupling.¹⁸

In the case of lactate racemase, mechanistic studies of the enzyme^{19,20} and synthetic model complexes^{21–23} have arrived at a proton-coupled hydride transfer mechanism²⁴ for the racemization of lactate. Current evidence points to the transfer of hydride to and from the carbenic ipso carbon.

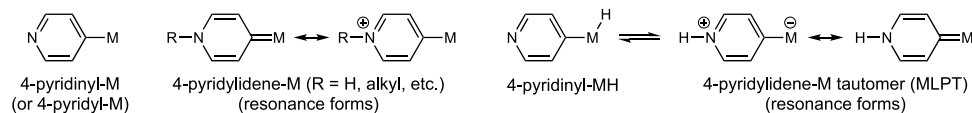
The influence of the metal upon pyridinyl ligands is demonstrated in the markedly enhanced basicity and nucleophilicity of 2-pyridinyl and 4-pyridinyl organometallic complexes compared with free pyridine,^{25–28} presumably a consequence of π -electron donation from the metal center. In the case of a metal hydride complex, this interaction would also be expected to increase its acidity. The combination of increased acidity of the hydride and high basicity at nitrogen raises the

Received: March 31, 2023

Published: August 8, 2023



Scheme 1. Pyridinyl and Pyridylidene Metal Complexes (Illustrated for Metalation at the 4-Position)



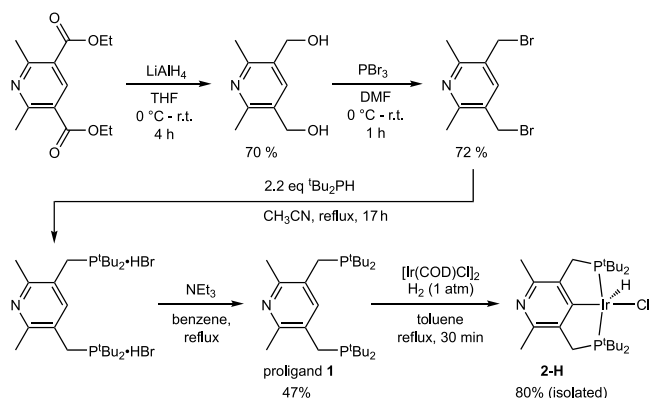
possibility of an interesting example of metal–ligand proton tautomerism (MLPT), a phenomenon that has achieved increasing recognition of late.^{29–31} In this case a metal hydride would interconvert with a lower oxidation state pyridylidene tautomer—alternatively formulated as a zwitterionic pyridyl complex with a formal negative charge on the metal (Scheme 1).

Beyond the pincer motif, there are a growing number of organometallic pyridinyl and pyridylidene complexes in the literature.^{5,12} However, there are no examples that include transition metal hydrides—or at least ones where the transition metal hydride is the dominant tautomer at equilibrium (examples of C–H activation alpha to a pyridyl nitrogen invariably prefer the pyridylidene tautomer at equilibrium^{32–38}).

In the present study, we find that metal–ligand proton tautomerism of a 4-lutidinyl pincer iridium hydride strongly favors its reaction with one-electron oxidants. Initial oxidation, in turn, leads to secondary proton and electron transfer, affording an unusual and highly reactive four-coordinate cationic Ir(III) complex. Ultimately, an intramolecular C(sp³)–H activation results, driven by proton and electron transfer, having been initiated by MLPT.³⁹

2. EXPERIMENTAL RESULTS

2.1. Synthesis and Characterization of 2-H. The 4-lutidinyl “PCP” proligand, pN-^tBuPCP-H (**1**), is prepared from the Hantzsch pyridine ethyl ester,⁴⁰ as depicted in Scheme 2 and described in the

Scheme 2. Synthesis of pN-^tBuPCP-H (**1**) and Metalation to Give 2-H

Supporting Information. X-ray quality crystals of proligand **1** were grown by slow evaporation from benzene; the crystallographically determined molecular structure is shown in Figure 1a. Refluxing a mixture of **1** with [Ir(COD)Cl]₂ (COD = 1,5-cyclooctadiene) in toluene under 1 atm hydrogen resulted in a change of the solution color from orange to cherry red within a few minutes, with metalation apparently complete within 30 min. Evaporation of the solvent under vacuum afforded an orange, microcrystalline, air-sensitive powder, **2-H** (Scheme 2). ¹H, ¹³C, and ³¹P NMR spectra of **2-H** are similar to those of (^tBuPCP)IrHCl (**3-H**),^{1,41} (*p*-NO₂-^tBuPCP)IrHCl,⁴² (*p*-MeO-^tBuPCP)IrHCl,⁴³ and (*p*-Me₂N-^tBuPCP)IrHCl.⁴⁴ In benzene-*d*₆, a hydride resonance appears as a triplet at –41.9 ppm (²J_{P–H} = 12 Hz) in the ¹H NMR spectrum. The phosphino-*t*-butyl groups as well as the methylene protons of the pincer arms are inequivalent in the ¹H NMR

spectrum; the *t*-butyl groups appear as two virtual triplets and the methylene protons appear as two doublets of virtual triplets. The selectively proton-decoupled ³¹P NMR spectrum shows a doublet at 68.8 ppm with a coupling to the hydride proton of ²J_{P–H} = 12 Hz. X-ray quality crystals of complex **2-H** were grown from pentane/toluene at –40 °C, and the XRD structure (Figure 1b) was consistent with the assignment based on NMR spectroscopy, although the hydride ligand was not unambiguously located.

2.2. Basicity of 2-H. To estimate the basicity of the remote nitrogen in complex **2-H**, a solution of 2,6-lutidinium chloride in DMSO (pK_a 4.46) was added to solid **2-H** (which is insoluble in DMSO). **2-H** was completely taken up into solution—indicating that the remote nitrogen was protonated by the 2,6-lutidinium salt. The resulting **2-H**•HCl is soluble in DMSO and water. However, when a solution of DBU•HCl in DMSO (pK_a = 13.9 in DMSO⁴⁵) is added to solid **2**, only some of the materials is taken into the solution, suggesting that pK_a of **2-H**•HCl is perhaps similar to that of DBU•HCl. Determination of the protonation equilibrium is confounded, however, by the heterogeneous nature of this reaction as well as possible coordination of solvent or chloride trans to the hydride in **2-H**•HCl. Computationally, using density functional theory (see details below and Supporting Information), the pyridinyl nitrogen of **2-H** is predicted to be 3.6 pK_a units more basic (in DMSO) than the corresponding nitrogen of **1** (Scheme 3).

2.3. Oxidations of 2-H. Orange-red solutions of complex **2-H** in noncoordinating solvents immediately turn dark purple upon exposure to air. This attracted our interest because the analogous “parent” complex bearing a phenyl-based PCP ligand, (^tBuPCP)IrHCl (**3-H**), and even analogues bearing π-donating para-substituents (methoxy⁴³ or dimethylamino⁴⁴) do not show similar air-sensitivity. We therefore investigated the oxidation of **2-H** with oxidants that generally afford simpler reactivity than O₂. Importantly, and consistent with the pronounced difference in air-sensitivity between **2-H** and **3-H**, those oxidants described below that are found to react rapidly with **2-H** (Table 1) undergo no reaction with **3-H** under the same conditions in the timeframe of the investigation.

2.3.1. Reaction of 2-H with Cp₂Fe⁺. When 1 equivalent of ferrocenium hexafluorophosphate is added to a solution of **2-H** in dichloromethane-*d*₂ the orange solution rapidly turns dark purple, followed by a slow conversion to light red. ³¹P and ¹H NMR spectroscopy reveals that **2-H** has undergone quantitative conversion. The ³¹P{¹H} NMR spectrum reveals the presence of two major species (Scheme 4).

One of the two major products observed is N-protonated, **2-H** (H⁺**2-H**; Scheme 4) which appears in the selectively decoupled ³¹P NMR spectrum as a doublet at 67.9 ppm, coupled (²J_{P–H} = 11.5 Hz) to a hydride at –40.5 ppm in the ¹H NMR spectrum. The phosphino-*t*-butyl groups appear as two overlapping virtual triplets at 1.37 ppm. The second set of signals in the ³¹P NMR spectrum comprises two doublets, at 49.8 and 8.7 ppm, with a strong mutual coupling of 345 Hz. ³¹P–¹H HMBC (see Supporting Information) was used to correlate the ³¹P NMR signal at 8.7 ppm with two doublets in the ¹H NMR spectrum at 1.59 and 0.88 ppm, each with integral 3, as well as with two broad apparent triplets at 1.67 and 3.30 ppm, each with integral 1 (attributable to the two methyl groups and the two methylene protons, respectively, of the cyclometalated *t*-butyl group). The doublet at 49.8 ppm in the ³¹P NMR spectrum correlates with two doublets in the ¹H NMR spectrum, each with integral 9, at 1.31 and 1.19 ppm. The presence of two overlapping signals at 10.66 and 10.57 ppm in a near 1:1 ratio in the ¹H NMR spectrum indicated the new products are both protonated at the pyridinyl nitrogen. These spectral features are characteristic of a cyclometalated pincer complex,^{43–50} in which one of the *t*-butyl groups of **2-H** has undergone C–H activation to form H⁺**4** (Scheme 4). Thus,

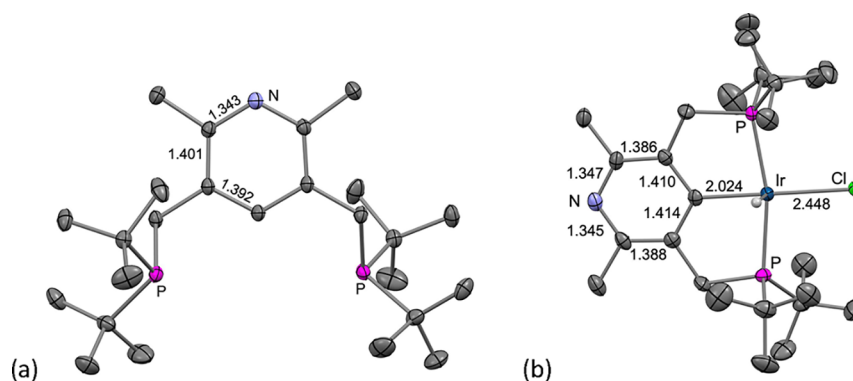
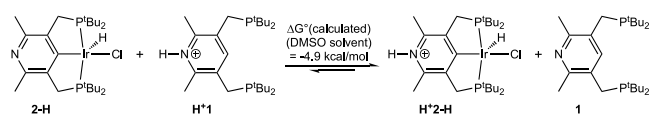


Figure 1. Molecular structures of (a) (pN-^tBuPCP-H) (**1**) and (b) (pN-^tBuPCP)IrHCl (**2-H**) determined by XRD. Hydrogen atoms, except for the hydride ligand, were omitted for clarity. Selected bond lengths in Å.

Scheme 3. Calculated Equilibrium Illustrating Increased Basicity of **1** upon Metalation



coupled with two one-electron oxidations and Ir–C bond formation, the hydride proton and a *t*-butyl proton of **2-H** have undergone net transfer to the pyridinyl nitrogen atoms of the now-cyclometalated complex **4** and another molecule of **2-H**.

The addition of *two* equivalents ferrocenium hexafluorophosphate to a solution of **2-H** in dichloromethane-*d*₂ also results in the orange solution rapidly turning dark purple followed by slow conversion to red, and ³¹P and ¹H NMR spectroscopy again reveals that **2-H** has undergone quantitative conversion. However, it appears that, while in this case, there are enough oxidizing equivalents to convert all **2-H** to **H*4**, the protonation of all pN-pyridinyl-PCP nitrogen upon reaction with one equiv. [Cp₂Fe]⁺[PF₆][−] (**Scheme 4**) inhibits further oxidation, and conversion to **H*4** is only 74%. Consistent with this hypothesis, in the presence of excess 2,6-lutidine (9 equiv), the reaction of two equiv. [Cp₂Fe]⁺[PF₆][−] with **2-H** results in nearly complete (90%) conversion to **H*4** upon mixing (**Scheme 5**).

2.3.2. Reaction of 2-H with Ph₃C⁺. Mixing complex **2-H** with 1 equivalent of [Ph₃C⁺][B(C₆F₅)₄[−]] (−0.11 V^{S1} vs Fc/Fc⁺) in dichloromethane-*d*₂ results in an instantaneous color change to dark purple. The solution then gradually lightens to orange. The ¹H NMR spectrum reveals a 0.7:1 ratio of **H*4** to **H*2-H**, along with a half equivalent of Gomberg's dimer ((Ph₃C)₂; **Scheme 6**). Thus, the trityl cation has acted as a single-electron oxidant, yielding approximately the same results as were obtained with 1 equivalent [Cp₂Fe⁺][PF₆].

2.3.3. Reactions of 2-H with Benzoquinone (BQ). The reaction of complex **2-H** with one equivalent of BQ leads to quantitative conversion to **4** and hydroquinone within 48 h at 22 °C (**Scheme 7**). Hydroquinone precipitates as a white solid from the reaction mixture. Following filtration, slow evaporation of the filtrate at ambient temperature produced crystals of complex **4**, the molecular structure of which was determined by XRD (**Figure 2**).

A paramagnetic intermediate is observed in the course of the reaction of **2-H** with BQ. Upon addition of **2-H** (7 mM) to BQ (540 mM) in benzene-*d*₆, the solution turns dark purple within 2 min of mixing. NMR reveals that approximately 50% of **2-H** has been converted to this paramagnetic species which has broad signals at −31 and 14.8 ppm in the ¹H NMR spectrum that integrates in a 1:6 ratio. This ratio allows assignment of the signals to the α -methyl groups and *t*-butyl groups, respectively. It follows then that this intermediate contains two mirror planes of symmetry, which renders all four *t*-butyl groups as well as the two α -methyl groups equivalent on the relevant NMR timescale. The methylene signals of the pincer arms in this paramagnetic intermediate were not observed and may be broadened into the baseline. These signals, assigned to Ir(II) complex **2•**, diminish with concomitant growth of signals attributable to **4** over the next 2 h (see **Supporting Information**).

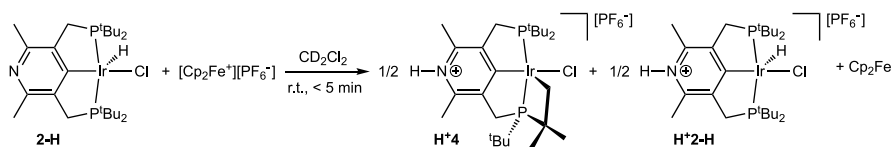
2.3.4. Chemical Characterization of the Paramagnetic Intermediate Resulting from the Initial Single-Electron Oxidations. In an effort to further characterize the paramagnetic intermediate, a solution of **2-H** (12 mM) in benzene-*d*₆ was allowed to react with only a slight excess (1.5 eq) of benzoquinone for 5 min at 25 °C; 29% conversion of **2-H** to the paramagnetic intermediate is observed by ¹H NMR (**Scheme 8**). A 4-fold excess of TEMPO-H (1-hydroxy-2,2,6,6-tetramethyl-piperidine)(O-H BDFE = 65.2 kcal/mol^{S2}) was then added to quench the paramagnetic species. The ¹H NMR spectrum taken immediately afterward indicated that **2-H** was the sole remaining

Table 1. Reaction of **2-H** with Various Oxidants

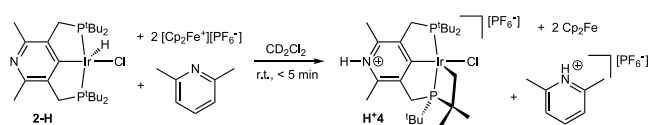
entry	[2-H] ₀ (mM)	oxidant	base	[H*4] (mM)	[H*2-H] (mM)
1	25	[Cp ₂ Fe ⁺][PF ₆ [−]] (1 eq)		16.3	8.6
2	13.3	[Cp ₂ Fe ⁺][PF ₆ [−]] (2 eq)		9.8	3.5
3	11.7	[Cp ₂ Fe ⁺][PF ₆ [−]] (2 eq)	2,6-lutidine (9 eq)	10.6 ^a	
4	12.5	[Ph ₃ C ⁺][B(C ₆ F ₅) ₄ [−]] (1 eq)		4.9	7.6
5	7	Benzoquinone (1 eq) ^b		1.9 ^{a,d}	
6	7	Benzoquinone (1 eq) ^c		5.5 ^{a,d}	
7	7.5	[(<i>p</i> -MeOC ₆ H ₄)Ph ₃ C ⁺][BF ₄ [−]] (2 eq)		no reaction	
8	11.1	[Cp* ₂ Fe ⁺][BF ₄ [−]] (2 eq) ^e		no reaction	

^aRemainder of mass balance is unreacted **2-H**. ^b40 min. ^c48 h. ^dProduct is complex **4**. ^eCp* = η⁵-C₅Me₅.

Scheme 4. Reaction of 2-H with 1 Equiv Ferrocenium Hexafluorophosphate



Scheme 5. Reaction of 2-H with 2 Equiv Ferrocenium Hexafluorophosphate and Lutidine



iridium-containing species in the solution (Scheme 8). On the basis of these data, the paramagnetic species 2^* is assigned as the four-coordinate product resulting from the loss of H from 2-H.

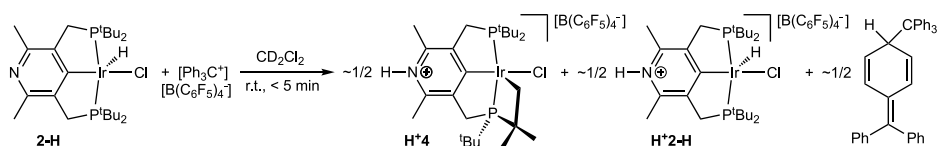
In accord with our assignment of 2^* , it was independently generated by the reaction of 2-H with the isolable tri-*t*-butylphenoxy radical^{S2–S4} (BDFE = 76.7 kcal/mol^{S2,S3}) (20% yield and conversion by ¹H NMR; Scheme 9).

3. MECHANISTIC CONSIDERATIONS AND DFT CALCULATIONS

3.1. Initial Oxidation of 2-H via MLPT. Based on the greater electronegativity of N than C, simple one-electron oxidation of 2-H is expected to be thermodynamically less favorable than oxidation of phenyl-based (^tBuPCP)IrHCl (3-H) or its 3,5-dimethylphenyl-based derivative 3'-H (which is even more closely analogous to 2-H). The results of DFT calculations are consistent with this simple reasoning: the ionization energy of 2-H is calculated to be 5.2 kcal/mol less favorable than that of 3'-H. In absolute terms, one-electron oxidation of 2-H by Cp₂Fe⁺ in CH₂Cl₂ is calculated to be endergonic by 14.0 kcal/mol. These values are in very good agreement with the results of cyclic voltammetry studies. The CV of 3-H shows a chemically irreversible oxidation wave at 0.33 V vs Fc^{0/+}, while that of 2-H has a chemically irreversible wave at 0.59 V vs Fc^{0/+} (Figure S40) which implies that direct oxidation of 2-H is 6.0 kcal/mol less favorable.

We calculate that 2-H can undergo transfer of H from Ir to the pyridinyl nitrogen; the resulting MLPT tautomer, 2-H-t, is 6.5 kcal/mol higher in free energy than 2-H. As shown in Figure 3 (top), there are two limiting resonance structures for the tautomer 2-H-t, one representing a zwitterionic form (2-H-t_{zwitter}) and one a carbene form (2-H-t_{carb}). A computed significant contraction of the Ir–C bond length (1.94 Å vs 2.03 Å for 2-H), and a more pronounced alternation of interatomic distance in the heterocyclic ring of 2-H-t compared with that of 2-H, implicates a significant contribution from resonance form 2-H-t_{carb} (Figure 3).

The low calculated free energy of tautomerization of 2-H, $\Delta G^{\circ}_{\text{MLPT}} = 6.5$ kcal/mol, is attributable to the relatively high acidity of the 2-H hydride, a result of the electron-withdrawing

Scheme 6. Reaction of 2 with 1 Equiv [Ph₃C⁺][B(C₆F₅)₄⁻]

Scheme 7. Reaction of 2 with 1 Equiv Benzoquinone

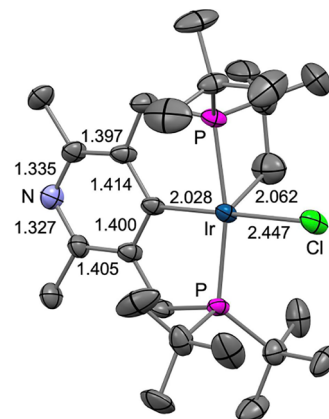
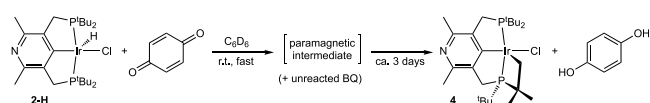
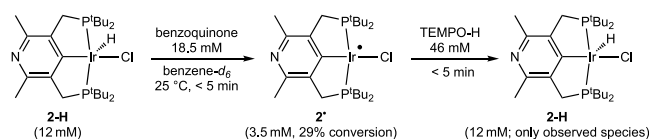
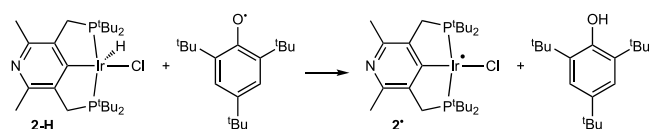


Figure 2. Molecular structure of 4 determined by XRD. H atoms omitted for clarity. Selected bond lengths in Å.

Scheme 8. Reaction of 2*, Generated In Situ, with TEMPO-H, to Give 2-H

Scheme 9. Reaction of 2-H with 2,4,6-^tBu₃C₆H₃O[•]

nature of the pyridinyl group, combined with the basicity of the pyridinyl nitrogen. The former effect is manifest by the calculated free energy of deprotonation of 2-H, 308.5 kcal/mol, which, for comparison, is 3.9 kcal/mol less than that of 3'-H and 5.1 kcal/mol less than that of (*p*-Me₂N-PCP)IrHCl. The high basicity of the pyridinyl nitrogen is reflected in its proton affinity being 10.7 kcal/mol greater than that of the dimethylamino group of (*p*-Me₂N-PCP)IrHCl. The pyridinyl

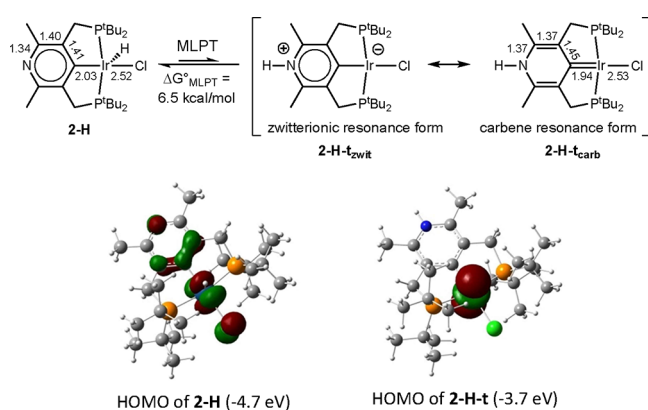


Figure 3. DFT-calculated structures and HOMOs of **2-H** and **2-H-t**. Bond lengths in Å.

N thus plays an unusual dual role of a group that is both quite basic and electron-withdrawing. The difference in $\Delta G^{\circ}_{\text{MLPT}}$ between **2-H** and (*p*-Me₂N-PCP)IrHCl (21.1 kcal/mol), however, is greater than even the sum of these two individual components (15.8 kcal/mol) would imply. This may be attributed to π -conjugation in tautomer **2-H-t** being more extensive than in **2-H**, as is suggested by the carbene resonance form **2-H-t_{carb}**. Accordingly, protonation of the N site of **2⁻** is 16.0 kcal/mol, more exergonic than that of (*p*-Me₂N-PCP)IrCl⁻ (compared with a difference of 10.7 kcal/mol for N-protonation of the respective neutral hydride complexes). These differences, and comparisons with (*p*-NO₂-PCP)IrHCl, a (pincer)IrHCl complex with a strongly electron-withdrawing substituent, are illustrated in Figure 4.⁵⁵

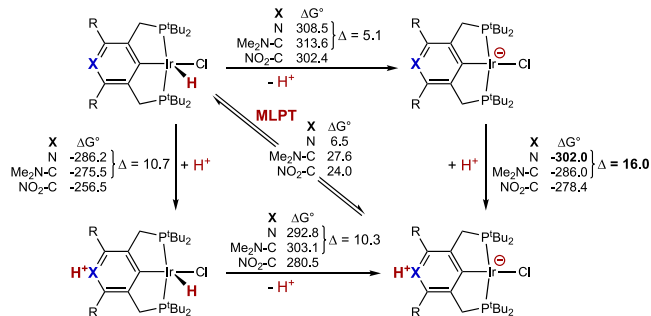


Figure 4. Thermochemical square scheme for MLPT calculated for **2-H** (R = Me) and (*p*-X-^tbuPCP)IrHCl (X = Me₂N and NO₂; R = H). Calculated Gibbs free energies at 298 K and 1 atm in kcal/mol, M06L-D3 in CH₂Cl₂ continuum. Differences (Δ) between **2-H** (R = Me) and (*p*-X-^tbuPCP)IrHCl (X = Me₂N), discussed in the text, specifically indicated.

One plausible pathway for the proposed MLPT would be via initial intermolecular proton transfer of the Ir–H proton of **2-H** to the nitrogen of a second **2-H** molecule. The barrier for this step is computed to be quite low (15.6 kcal/mol, Figure 5). Proton transfer initially gives an ion pair that can rearrange to deliver the proton to the nitrogen site of the deprotonated molecule of **2-H**, thereby affording **2-H-t**.

While tautomerization of **2-H** to give **2-H-t** is endergonic by only 6.5 kcal/mol, the oxidation of **2-H-t** by Cp₂Fe⁺ is calculated to be very favorable ($\Delta G^{\circ}_{\text{ox}} = -17.3$ kcal/mol). Thus, MLPT of **2-H** favors oxidation by a remarkable extent of 31.3 kcal/mol ($\Delta\Delta G^{\circ}_{\text{ox}}$ Figure 5). For purposes of qualitatively understanding this effect, it is perhaps convenient to consider the zwitterionic

resonance form **2-H-t_{zwit}**. The parent complex **2-H** has a d⁶ Ir(III) center and a HOMO derived largely from the metal 5d_{xz} orbital (Figure 3). MLPT to give **2-H-t_{zwit}** creates a square planar complex with a d⁸ Ir(I) center having a formally negative charge and a 5d_{z²} HOMO that is 1.0 eV higher than the HOMO in **2-H** (Figure 3). The reductive nature of MLPT with respect to the metal thereby explains the greatly more favorable oxidation of **2-H-t** relative to **2-H**.

Note that the difference in the oxidation energies of **2-H** and **2-H-t** ($\Delta\Delta G^{\circ}_{\text{ox}} = -31.3$ kcal/mol) is necessarily equal to the difference in the tautomerization energies of **2-H** and its oxidized form [**2-H**]^{•+} ($-\Delta\Delta G^{\circ}_{\text{MLPT}}$). Thus, in contrast with the parent complex **2-H**, MLPT of the radical cation [**2-H**]^{•+} is highly exergonic ($\Delta G^{\circ}_{\text{MLPT}} = -24.8$ kcal/mol; Figure 5). This may be viewed in terms of the increased metal oxidation state and the increased electric charge greatly increasing the acidity of the IrH bond in [**2-H**]^{•+} relative to **2-H** (with an expected decrease of at least 15 pK_a units^{56,57}), while having a much smaller effect on the basicity of the nitrogen which is distant from the center of oxidation. Thus, upon oxidation, the nitrogen becomes the favored site for the proton.

For a given molecule, $\Delta G^{\circ}_{\text{MLPT}}$ is equal to the difference between the Ir–H and N–H BDFEs. Similar to the acidity, the N–H BDFE in **2-H-t** is not expected to greatly change upon oxidation. Thus, the large change in $\Delta G^{\circ}_{\text{MLPT}}$ implies that the BDFE of the Ir–H bond in **2-H** is greatly weakened upon oxidation.

Oxidation of **2-H-t** generates the free radical cation **2-H-t^{•+}**. Subsequent deprotonation of **2-H-t^{•+}** by an unreacted molecule of **2-H** is computed to be essentially ergoneutral ($\Delta G^{\circ} = -0.1$ kcal/mol), yielding the d⁷ Ir(II) complex **2[•]**, our assignment for the paramagnetic intermediate observed in the reaction with benzoquinone (Schemes 7 and 8). The net energy of the formation of **2[•]** and H⁺**2-H** from two molecules of **2-H** and ferrocenium is computed to be quite negative, $\Delta G^{\circ} = -10.9$ kcal/mol. MLPT thereby enables a facile path for net “H-abstraction” from a metal hydride, **2-H**, via one-electron oxidation. The calculations in the next section show that oxidation of **2[•]** by another ferrocenium is viable and that it triggers intramolecular C–H activation.

3.2. Oxidation of 2[•] and Intramolecular C–H Activation. Oxidation of the Ir(II) complex **2[•]** by a second equivalent of ferrocenium is calculated to be only slightly endergonic ($\Delta G^{\circ} = 7.9$ kcal/mol). We calculated two minima, with nearly identical energies, for the resulting four-coordinate d⁶ cation. One of these has a square planar geometry with a triplet spin state (**3²⁺**), while the other has a seesaw geometry with a closed shell singlet state (**2⁺_{bent}**). **2⁺_{bent}** features an agostic C–H bond from a phosphino-*t*-butyl group donating into the otherwise empty orbital of the metal, with Ir–H and Ir–C bond distances of 2.08 and 2.81 Å.⁵⁸ For the triplet state, no minimum with an agostic bond could be located which is not surprising given that this state has no empty metal d atomic orbital.

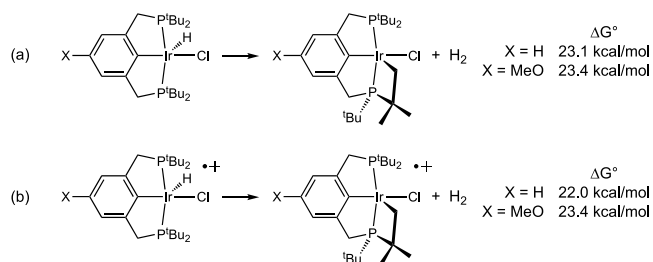
Oxidative cleavage of the agostic C–H bond of **2⁺_{bent}** is computed to proceed readily ($\Delta G^{\ddagger} = 14.4$ kcal/mol). The transition state⁵⁹ TS-**2⁺_{bent}** has a geometry characterized by a nearly (but not quite) complete C–H bond cleavage (*d* = 1.65 Å) and large degree of Ir–H (1.56 Å) and Ir–C (2.22 Å) bond formation. TS-**2⁺_{bent}** leads to the six-coordinate cyclometalated species **4-H⁺** which is calculated to be extremely acidic. Proton transfer from **4-H⁺** to the pyridinyl nitrogen of a second, neutral, molecule of **2-H**, to afford the observed metallacycle product **4** is highly exergonic ($\Delta G^{\circ} = -36.6$ kcal/mol). However, the proton

4. CONSIDERATIONS OF SELECTIVITY AND IMPLICATIONS FOR CATALYSIS

As discussed above, unlike the unsubstituted parent pincer complex (^tBuPCP)IrHCl, **3-H**, or derivatives, the para-pyridyl-based **2-H** reacts rapidly at ambient temperature with oxidants including O₂, trityl cation, ferrocenium, and benzoquinone. We attribute the facile oxidation of **2-H** to a preceding MLPT reaction. The equilibrium of the MLPT reaction lies toward **2-H** rather than **2-H-t**. This stands in contrast to 2-pyridinyl^{64,65} and imidazolyl metal hydride complexes^{32,33,36} where proton transfer from metal to ligand is favored at equilibrium. Recently, Kuo and Goldberg have reported an iridium pincer system, based on a bis(pyrazolyl)pyridine ligand, in which both Ir(III)-H and (L-H)Ir(I) tautomers are observable.²⁹ But while the formation of **2-H-t** is calculated to be slightly endergonic ($\Delta G^\circ = 6.5$ kcal/mol), DFT calculations predict that its oxidation is far more favorable than that of **2-H** (by 31.3 kcal/mol), to give **H⁺2⁺** which is then deprotonated to give **2⁺**. Oxidation of the resulting Ir(II) complex **2⁺** is calculated to yield intermediate, **2⁺_{bent}**, which is calculated to readily insert into an sp³ C–H bond of a phosphino-*t*-butyl group to produce the highly acidic species **4-H⁺**, which upon deprotonation gives the observed cyclometalated complex **4**. The oxidation of **2-H-t** is not observed by CV since its equilibrium concentration at the electrode is too small.

It is possible that cationic, d⁶ pincer iridium complexes similar to **2⁺_{bent}** have been involved in prior examples of cyclometalation reactions without being identified. For example, Koridze and coworkers reported that treatment of (^tBuPOCOP)IrHCl and (EtO₂C-^tBuPOCOP)IrHCl with trifluoroacetic acid leads to cyclometalation with loss of H₂.⁴⁹ Mayer and coworkers undertook cyclic voltammetry studies of (^tBuPCP)IrHCl and (MeO-^tBuPCP)IrHCl, in which they found that oxidation leads to cyclometalation with loss of H₂.^{43,66,67} They proposed that upon one-electron oxidation, cyclometalation to yield H₂ (Scheme 10, eq b) becomes thermodynamically favorable.

Scheme 10. Thermodynamics of Dehydrogenative Cyclometalation of (X-^tBuPCP)IrHCl and Their Corresponding One-Electron Oxidation Products



Our calculations, however, strongly indicate that the thermodynamics of such dehydrogenative cyclometalation reactions are substantially endergonic and strikingly unaffected by single-electron oxidation (Scheme 10).

It is important to note that [(pN-^tBuPCP)Ir(III)Cl]⁺, **2⁺**, undergoes intramolecular C–H activation, in contrast with Ir(I) complexes of isostructural ^tBuPCP or ^tBuPOCOP ligands which are among the most well-known complexes for intermolecular C–H activation (and functionalization).^{68–70} The different reactivity is undoubtedly not based on electronic factors; the C–H bond of a *t*-butyl group is certainly not very different than that of an *n*-alkane, with respect to electronic factors, in any way that

would strongly bias its relative reactivity toward an Ir(III) versus an Ir(I) center. Presumably the preference of the Ir(III) species to undergo intramolecular C–H addition, in contrast with the Ir(I) fragments, is based on the very different geometries and steric environments of the respective vacant coordination sites that enable the C–H addition reactions. Specifically, the active site in the case of (pincer)Ir(I) complexes is trans to the pincer aryl carbon, as compared to a site cis to the analogous carbon in the case of [(pN-^tBuPCP)Ir(III)Cl]⁺. The trans site of (PCP)Ir(I) complexes is significantly less crowded than the cis sites,⁷¹ allowing intermolecular access to an alkane. Conversely, the coordination site cis to the pincer ipso carbon is easily accessible to a phosphino-*t*-butyl group, while cyclometalation, in contrast with intermolecular C–H activation (in this case or generally^{72,73}), is not disfavored by crowding.

Calculations were conducted with the parent fragment (^tBuPCP)IrCl (**3**) to explore and quantify the proposed role of steric factors and the ligand architecture. Cyclometalation by **3⁺** (coupled with deprotonation by triethylamine as a model base) is found to be 9.5 kcal/mol more exergonic than the addition of a propane primary bond,^{74,75} while the kinetic barrier to cyclometalation, ΔG^\ddagger , is also (somewhat coincidentally) 9.5 kcal/mol less (Figure 7). In contrast, for the less crowded diisopropyl-phosphino analogue, (ⁱPrPCP)IrCl⁺, cyclometalation is calculated to have a kinetic barrier very slightly greater ($\Delta\Delta G^\ddagger = 0.3$ kcal/mol) than the barrier to the addition of a propane primary bond (which is calculated to be quite low, $\Delta G^\ddagger = 14.6$ kcal/mol). Thus, in comparing [(^tBuPCP)IrCl]⁺ versus [(ⁱPrPCP)IrCl]⁺, the calculated difference in selectivity for intermolecular versus intramolecular C–H activation is quite pronounced, 9.8 kcal/mol (expressed as $\Delta\Delta\Delta G^\ddagger$; Figure 7). The thermodynamic preference for cyclometalation by **3⁺** versus intermolecular C–H addition is also much greater than for (ⁱPrPCP)IrCl⁺, $\Delta\Delta G^\circ = -9.5$ kcal/mol versus -1.9 kcal/mol ($\Delta\Delta\Delta G^\circ = 7.6$ kcal/mol).

The reversal of selectivity in C–H activation, from intramolecular to intermolecular by the simple substitution of *i*-Pr groups for *t*-Bu groups, demonstrates that the observation of cyclometalation does not reflect an intrinsic tendency of cationic Ir(III) centers to necessarily undergo cyclometalation. This has important implications for exploiting, for catalytic applications, the unusual reactivity described in this work. For example, successive oxidations and loss of a proton from a more cyclometalation-resistant analogue of **2-H**, if followed by the addition of an *n*-alkyl C–H bond which would yield a species analogous to **4**, of the general form (PCP)IrCl(*n*-alkyl). β -H elimination by this 16-electron species, in analogy with the well-known behavior of (PCP)IrH(*n*-alkyl) complexes,^{68–70} would return the hydride reactant; in the case of (ⁱPrPCP)IrCl(*n*-Pr), the calculated barrier, ΔG^\ddagger , is a modest 17.9 kcal/mol (Scheme 11). These reactions would comprise a catalytic cycle for alkane dehydrogenation, driven by two proton-coupled electron transfers.

One could envision this by applying in an electrochemical system or a purely chemical system driven by O₂ as the ultimate oxidant (directly, or indirectly as in the case of the Wacker reaction system⁷⁶). We have previously reported that (^tBuPCP)-IrH₂ can catalyze PCET-driven alkane dehydrogenation;⁷⁷ however, that catalyst operates via an Ir(I) species which is subject to overoxidation, and thus far it requires a strong base for deprotonation. The high-oxidation-state cycle envisioned here might circumvent either or both of these issues.

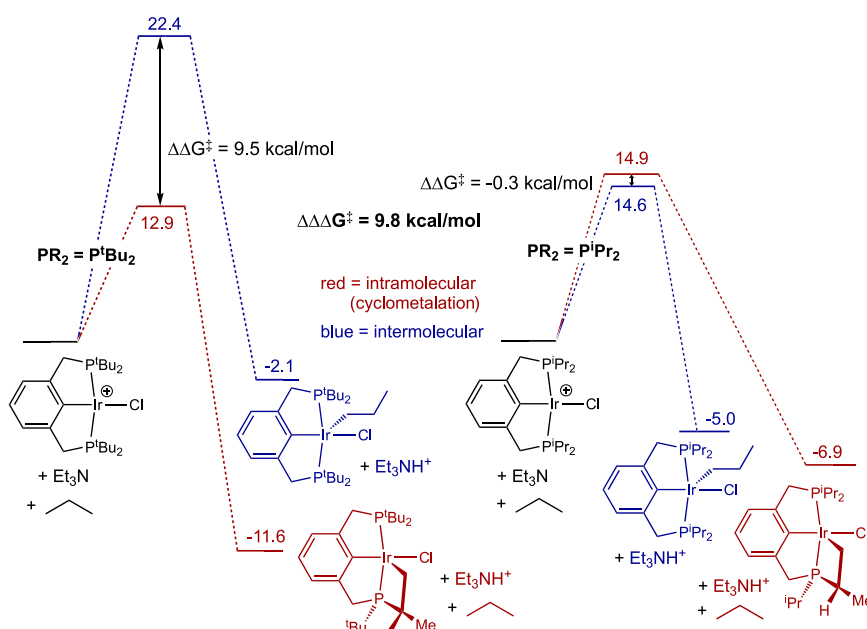
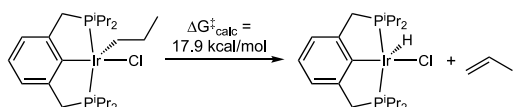


Figure 7. Free energies (kcal/mol) of intramolecular (cyclometalation) versus intermolecular C–H activation by $(R^4\text{PCP})\text{IrCl}^+$; R = $i\text{Pr}$ and $i\text{Bu}$; M06L-D3 in *n*-heptane continuum (Et_3N used as a model base; the choice of base has no effect on values of ΔG^\ddagger or relative values of ΔG°).

Scheme 11. β -H-Elimination by (Hypothetical) Product of C–H Addition/Deprotonation by $(i\text{Pr})\text{PCP IrCl}^+$



5. CONCLUSIONS

$(\text{pN-}i\text{BuPCP})\text{IrHCl}$, **2-H**, is intrinsically more difficult to oxidize (i.e., has a higher oxidation potential or free energy of one-electron oxidation) than the phenyl-based analogue ($i\text{BuPCP}$)- IrHCl or the even more closely related derivative, **3'-H**. Nevertheless, **2-H** displays much greater reactivity with oxidants including ferrocenium, trityl cation, and benzoquinone, as well as O_2 .

DFT calculations reveal the key intermediacy of an Ir(I) tautomer, resulting from MLPT, which can be characterized as either a zwitterion or a remote NHC complex. This tautomer is subject to facile one-electron oxidation to give the net loss of a hydrogen atom from the iridium center. The resulting product is a cationic N-protonated iridium(II) complex $\text{H}^+\mathbf{2}^\bullet$. Deprotonation then gives $\mathbf{2}^\bullet$, which is also fairly easily oxidized, to give $\mathbf{2}^+$, completing the net loss of a hydride from **2-H**. The 4-coordinate d^6 iridium complex $\mathbf{2}^+$ is calculated to undergo cyclometalation/C–H addition to give the strongly acidic complex $\mathbf{4-H}^+$. Loss of a proton from $\mathbf{4-H}^+$ gives the observed cyclometalated iridium(III) complex **4**.

PCP-type pincer ligands have yielded a very rich manifold of chemistry, particularly for the activation of small molecules and especially C–H bonds.^{68–70} The para-pyridyl pincer ligand appears to add a new dimension to this manifold by allowing the low-energy deprotonation of the metal center of a hydride complex, via MLPT. In this work, we see that such deprotonation facilitates oxidation, leading to the net loss of $\text{H}\bullet$ and ultimately H^- , to give a highly reactive coordinatively unsaturated cationic metal center.

ASSOCIATED CONTENT

Supporting Information

The Supporting Information is available free of charge at <https://pubs.acs.org/doi/10.1021/jacs.3c03376>.

Complete experimental details and synthetic procedures, NMR data, computational details, computed energies and thermodynamic quantities (PDF)

Optimized structures for calculated species (.mol format) (ZIP)

Accession Codes

CCDC 2215473–2215474 and 2254296 contain the supplementary crystallographic data for this paper. These data can be obtained free of charge via www.ccdc.cam.ac.uk/data_request/cif, or by emailing data_request@ccdc.cam.ac.uk, or by contacting The Cambridge Crystallographic Data Centre, 12 Union Road, Cambridge CB2 1EZ, UK; fax: +44 1223 336033.

AUTHOR INFORMATION

Corresponding Authors

Faraj Hasanayn – Department of Chemistry, American University of Beirut, Beirut 1107 2020, Lebanon; orcid.org/0000-0003-3308-7854; Email: fh19@aub.edu.lb

Alan S. Goldman – Department of Chemistry and Chemical Biology, Rutgers, The State University of New Jersey, Piscataway, New Jersey 08854, United States; Centre for Nanotechnology, Indian Institute of Technology Guwahati, Guwahati 781039 Assam, India; orcid.org/0000-0002-2774-710X; Email: alan.goldman@rutgers.edu

Authors

Tariq M. Bhatti – Department of Chemistry and Chemical Biology, Rutgers, The State University of New Jersey, Piscataway, New Jersey 08854, United States

Akshai Kumar – Centre for Nanotechnology, Indian Institute of Technology Guwahati, Guwahati 781039 Assam, India; orcid.org/0000-0002-3911-3630

Ashish Parihar – Department of Chemistry and Chemical Biology, Rutgers, The State University of New Jersey, Piscataway, New Jersey 08854, United States

Hellan K. Moncy – Department of Chemistry and Chemical Biology, Rutgers, The State University of New Jersey, Piscataway, New Jersey 08854, United States

Thomas J. Emge – Department of Chemistry and Chemical Biology, Rutgers, The State University of New Jersey, Piscataway, New Jersey 08854, United States

Kate M. Waldie – Department of Chemistry and Chemical Biology, Rutgers, The State University of New Jersey, Piscataway, New Jersey 08854, United States; orcid.org/0000-0001-6444-6122

Complete contact information is available at:
<https://pubs.acs.org/10.1021/jacs.3c03376>

Notes

The authors declare no competing financial interest.

ACKNOWLEDGMENTS

This work was supported by the U.S. Department of Energy Office of Science (DE-SC0020139). F.H. thanks AUB for supporting a Sabbatical leave spent at Rutgers. We acknowledge the Office of Advanced Research Computing (OARC) at Rutgers and the HPC center at AUB for providing computational resources.

REFERENCES

- (1) Moulton, C. J.; Shaw, B. L. Transition Metal-Carbon Bonds. Part XLII. Complexes of Nickel, Palladium, Platinum, Rhodium and Iridium with the Tridentate Ligand 2,6-bis[(di-tert-butylphosphino)methyl]phenyl. *J. Chem. Soc., Dalton Trans.* **1976**, 1020–1024.
- (2) Fraser, P. J.; Roper, W. R.; Stone, F. G. A. Carbene complexes of iridium, rhodium, manganese, chromium, and iron containing thiazolidinylidene and pyridinylidene ligands. *J. Chem. Soc., Dalton Trans.* **1974**, 760–764.
- (3) Desguin, B.; Zhang, T.; Soumillion, P.; Hols, P.; Hu, J.; Hausinger, R. P. A tethered niacin-derived pincer complex with a nickel-carbon bond in lactate racemase. *Science* **2015**, 349, 66–69.
- (4) Xu, T.; Bauer, G.; Hu, X. A Novel Nickel Pincer Complex in the Active Site of Lactate Racemase. *ChemBioChem* **2016**, 17, 31–32.
- (5) Schuster, O.; Yang, L.; Raubenheimer, H. G.; Albrecht, M. Beyond Conventional N-Heterocyclic Carbenes: Abnormal, Remote, and Other Classes of NHC Ligands with Reduced Heteroatom Stabilization. *Chem. Rev.* **2009**, 109, 3445–3478.
- (6) Strasser, C. E.; Stander-Grobler, E.; Schuster, O.; Cronje, S.; Raubenheimer, H. G. Preparation of Remote NHC Complexes of Rhodium(I) and Gold(I) by Ligand Transfer. *Eur. J. Inorg. Chem.* **2009**, 2009, 1905–1912.
- (7) Heydenrych, G.; von Hopffgarten, M.; Stander, E.; Schuster, O.; Raubenheimer, H. G.; Frenking, G. The Nature of the Metal–Carbene Bond in Normal and Abnormal Pyridylidene, Quinolyidene and Isoquinolyidene Complexes. *Eur. J. Inorg. Chem.* **2009**, 2009, 1892–1904.
- (8) Alvarez, E.; Hernandez, Y. A.; Lopez-Serrano, J.; Maya, C.; Paneque, M.; Petronilho, A.; Poveda, M. L.; Salazar, V.; Vattier, F.; Carmona, E. Metallacyclic Pyridylidene Structures from Reactions of Terminal Pyridylidenes with Alkenes and Acetylene. *Angew Chem., Int. Ed.* **2010**, 49, 3496–3499, S3496/3491–S3496/3438, DOI: 10.1002/anie.201000608.
- (9) Segarra, C.; Mas-Marza, E.; Mata, J. A.; Peris, E. Rhodium and Iridium Complexes with Chelating C-C'-Imidazolylidene-Pyridylidene Ligands: Systematic Approach to Normal Abnormal, and Remote Coordination Modes. *Organometallics* **2012**, 31, 5169–5176.
- (10) Bajo, S.; Esteruelas, M. A.; Lopez, A. M.; Onate, E. Alkenylation of 2-methylpyridine via pyridylidene-osmium complexes. *Organometallics* **2012**, 31, 8618–8626.
- (11) Albrecht, M. In *Adv. Organomet. Chem.*; Pérez, P. J., Ed.; Academic Press, 2014; Vol. 62, pp 111–158.
- (12) Vivancos, A.; Segarra, C.; Albrecht, M. Mesoionic and Related Less Heteroatom-Stabilized N-Heterocyclic Carbene Complexes: Synthesis, Catalysis, and Other Applications. *Chem. Rev.* **2018**, 118, 9493–9586.
- (13) Schneider, S. K.; Julius, G. R.; Loschen, C.; Raubenheimer, H. G.; Frenking, G.; Herrmann, W. A. A first structural and theoretical comparison of pyridinylidene-type rNHC (remote N-heterocyclic carbene) and NHC complexes of Ni(II) obtained by oxidative substitution. *Dalton Trans.* **2006**, 1226–1233.
- (14) Crociani, B.; Dibianca, F.; Bertani, R.; Castellani, C. B. Insertion of isocyanides into the palladium–carbon bond of C2-palladated heterocycles. Synthesis of trans-[PdCl{C(RN)=NR}(PPh₃)₂] complexes (RN = 2-pyridyl, 2-pyrazyl; R = alkyl or aryl group) *Inorg. Theor. Chim. Acta* **1985**, 101, 161–169.
- (15) Crociani, B.; Di Bianca, F.; Giovenco, A.; Berton, A. N-protonated 2-pyridylnickel(II) complexes insertion of isocyanides into the nickel–2-pyridyl bond. *J. Organomet. Chem.* **1987**, 323, 123–134.
- (16) Swisher, N. A.; Grubbs, R. H. Synthesis and Characterization of 3,5-Bis(di-tert-butylphosphinito)pyridine Pincer Complexes. *Organometallics* **2020**, 39, 2479–2485.
- (17) Horak, K. T.; VanderVelde, D. G.; Agapie, T. Tuning of Metal Complex Electronics and Reactivity by Remote Lewis Acid Binding to π -Coordinated Pyridine Diphosphine Ligands. *Organometallics* **2015**, 34, 4753–4765.
- (18) Tang, S.; von Wolff, N.; Diskin-Posner, Y.; Leitus, G.; Ben-David, Y.; Milstein, D. Pyridine-Based PCP-Ruthenium Complexes: Unusual Structures and Metal–Ligand Cooperation. *J. Am. Chem. Soc.* **2019**, 141, 7554–7561.
- (19) Zhang, X.; Chung, L. W. Alternative Mechanistic Strategy for Enzyme Catalysis in a Ni-Dependent Lactate Racemase (LarA): Intermediate Destabilization by the Cofactor. *Chem. – Eur. J.* **2017**, 23, 3623–3630.
- (20) Wang, B.; Shaik, S. The Nickel-Pincer Complex in Lactate Racemase Is an Electron Relay and Sink that acts through Proton-Coupled Electron Transfer. *Angew Chem., Int. Ed.* **2017**, 56, 10098–10102.
- (21) Xu, T.; Wodrich, M. D.; Scopelliti, R.; Corminboeuf, C.; Hu, X. Nickel pincer model of the active site of lactate racemase involves ligand participation in hydride transfer. *Proc Natl. Acad. Sci. U. S. A.* **2017**, 114, 1242–1245.
- (22) Shi, R.; Wodrich, M. D.; Pan, H.-J.; Tirani, F. F.; Hu, X. Functional Models of the Nickel Pincer Nucleotide Cofactor of Lactate Racemase. *Angew Chem., Int. Ed.* **2019**, 58, 16869–16872.
- (23) Qiu, B.; Yang, X. A bio-inspired design and computational prediction of scorpion-like SCS nickel pincer complexes for lactate racemization. *Chem. Commun.* **2017**, 53, 11410–11413.
- (24) Rankin, J. A.; Mauban, R. C.; Fellner, M.; Desguin, B.; McCracken, J.; Hu, J.; Varganov, S. A.; Hausinger, R. P. Lactate Racemase Nickel-Pincer Cofactor Operates by a Proton-Coupled Hydride Transfer Mechanism. *Biochemistry* **2018**, 57, 3244–3251.
- (25) Canovese, L.; Visentin, F.; Uguagliati, P.; Di Bianca, F.; Fontana, A.; Crociani, B. Organometallic nucleophiles. A mechanistic study of halide displacement at saturated carbon by 2- and 4-pyridyl complexes of palladium(II) and platinum(II). *J. Organomet. Chem.* **1996**, 525, 43–48.
- (26) Canovese, L.; Uguagliati, P.; Di Bianca, F.; Crociani, B. Organometallic nucleophiles. Mechanism of halide displacement at saturated carbon by 2-pyridyl and 4-pyridyl complexes [M(dmct)-(C₅H₄N-Cn)(L)] (M = Pd, Pt; dmct = dimethyldithiocarbamate; n = 2,4; L = tertiary phosphine). *J. Organomet. Chem.* **1992**, 438, 253–263.
- (27) Crociani, B.; Di Bianca, F.; Uguagliati, P.; Canovese, L. A powerful organometallic nucleophile the 2-pyridyl group in (dimethyldithio-carbamate) (2-pyridyl)(triphenyl-phosphine)platinum(II). *Inorg. Chim. Acta* **1990**, 176, 5–6.

- (28) Crociani, B.; di Bianca, F.; Giovenco, A.; Scrivanti, A. Protonation and methylation reactions of 2-pyridyl-palladium(II) and -platinum(II) complexes. *J. Organomet. Chem.* **1983**, *251*, 393–411.
- (29) Kuo, J. L.; Goldberg, K. I. Metal/Ligand Proton Tautomerism Facilitates Dinuclear H₂ Reductive Elimination. *J. Am. Chem. Soc.* **2020**, *142*, 21439–21449.
- (30) Jain, A. K.; Gau, M. R.; Carroll, P. J.; Goldberg, K. I. Comparing Square-Planar Rh^I and Ir^I: Metal–Ligand Proton Tautomerism Fluxionality, and Reactivity. *Organometallics* **2022**, *41*, 3341–3348.
- (31) Jain, A. K.; Gau, M. R.; Carroll, P. J.; Goldberg, K. I. The underappreciated influence of ancillary halide on metal–ligand proton tautomerism. *Chem. Sci.* **2022**, *13*, 7837–7845.
- (32) Esteruelas, M. A.; Fernández-Alvarez, F. J.; Oñate, E. Stabilization of NH Tautomers of Quinolines by Osmium and Ruthenium. *J. Am. Chem. Soc.* **2006**, *128*, 13044–13045.
- (33) Esteruelas, M. A.; Fernández-Alvarez, F. J.; Oñate, E. Osmium and Ruthenium Complexes Containing an N-Heterocyclic Carbene Ligand Derived from Benzo[h]quinoline. *Organometallics* **2007**, *26*, 5239–5245.
- (34) Esteruelas, M. A.; Fernandez-Alvarez, F. J.; Olivan, M.; Onate, E. NH-Tautomerization of Quinolines and 2-Methylpyridine Promoted by a Hydride-Iridium(III) Complex: Importance of the Hydride Ligand. *Organometallics* **2009**, *28*, 2276–2284.
- (35) Buil, M. L.; Esteruelas, M. A.; Garces, K.; Olivan, M.; Onate, E. C_β (sp²)-H Bond Activation of alpha, beta -Unsaturated Ketones Promoted by a Hydride-Elongated Dihydrogen Complex: Formation of Osmafuran Derivatives with Carbene Carbyne, and NH-Tautomerized alpha -Substituted Pyridine Ligands. *Organometallics* **2008**, *27*, 4680–4690.
- (36) Wiedemann, S. H.; Lewis, J. C.; Ellman, J. A.; Bergman, R. G. Experimental and Computational Studies on the Mechanism of N-Heterocycle C-H Activation by Rh(I). *J. Am. Chem. Soc.* **2006**, *128*, 2452–2462.
- (37) Lewis, J. C.; Berman, A. M.; Bergman, R. G.; Ellman, J. A. Rh(I)-Catalyzed Arylation of Heterocycles via C-H Bond Activation: Expanded Scope through Mechanistic Insight. *J. Am. Chem. Soc.* **2008**, *130*, 2493–2500.
- (38) Lewis, J. C.; Bergman, R. G.; Ellman, J. A. Rh(I)-Catalyzed Alkylation of Quinolines and Pyridines via C-H Bond Activation. *J. Am. Chem. Soc.* **2007**, *129*, 5332–5333.
- (39) A preprint of this work has been published on ChemRxiv: Bhatti, T. M.; Kumar, A.; Parihar, A.; Emge, T. J.; Hasanayn, F.; Goldman, A. S. Metal-Ligand Tautomerism, Electron-Transfer, and C(sp³)-H Activation by a 4 Pyridinyl-Pincer Iridium Hydride Complex. *ChemRxiv* **2023**, DOI: 10.26434/chemrxiv-2021-mqjrc.
- (40) Joule, J. A.; Mills, K. In *Heterocyclic Chemistry*, 5th ed.; John Wiley & Sons: West Sussex, UK, 2010, pp 158–162.
- (41) Punji, B.; Emge, T. J.; Goldman, A. S. A Highly Stable Adamantyl-Substituted Pincer-Ligated Iridium Catalyst for Alkane Dehydrogenation. *Organometallics* **2010**, *29*, 2702–2709.
- (42) Grimm, J. C.; Nachtigal, C.; Mack, H. G.; Kaska, W. C.; Mayer, H. A. A novel functionalized P,C,P pincer ligand complex. *Inorg. Chem. Commun.* **2000**, *3*, 511–514.
- (43) Mohammad, H. A. Y.; Grimm, J. C.; Eichele, K.; Mack, H.-G.; Speiser, B.; Novak, F.; Quintanilla, M. G.; Kaska, W. C.; Mayer, H. A. C-H Oxidative Addition with a (PCP)Ir(III)-Pincer Complex. *Organometallics* **2002**, *21*, 5775–5784.
- (44) Huang, Z.; Brookhart, M.; Goldman, A. S.; Kundu, S.; Ray, A.; Scott, S. L.; Vicente, B. C. Highly Active and Recyclable Heterogeneous Iridium Pincer Catalysts for Transfer Dehydrogenation of Alkanes. *Adv. Synth. Catal.* **2009**, *351*, 188–206.
- (45) Kütt, A.; Selberg, S.; Kaljurand, I.; Tshepelevitsh, S.; Heering, A.; Darnell, A.; Kaupmees, K.; Piirsalu, M.; Leito, I. pK_a values in organic chemistry – Making maximum use of the available data. *Tetrahedron Lett.* **2018**, *59*, 3738–3748.
- (46) Kundu, S.; Choi, J.; Wang, D. Y.; Choliy, Y.; Emge, T. J.; Krogh-Jespersen, K.; Goldman, A. S. Cleavage of Ether, Ester, and Tosylate C(sp³)-O Bonds by an Iridium Complex, Initiated by Oxidative Addition of C-H Bonds. Experimental and Computational Studies. *J. Am. Chem. Soc.* **2013**, *135*, 5127–5143.
- (47) Lokare, K. S.; Nielsen, R. J.; Yousufuddin, M.; Goddard, W. A., III; Periana, R. A. Iridium complexes bearing a PNP ligand, favoring facile C(sp³)-H bond cleavage. *Dalton Trans.* **2011**, *40*, 9094–9097.
- (48) Isobe, K.; Nakamura, Y.; Miwa, T.; Kawaguchi, S. Comparative Studies of 2-, 3-, and 4-Pyridylpalladium(II) Complexes: Synthesis and Properties. *Bull. Chem. Soc. Jpn.* **1987**, *60*, 149–157.
- (49) Polukeev, A. V.; Kuklin, S. A.; Petrovskii, P. V.; Peregudov, A. S.; Dolgushin, F. M.; Ezernitskaya, M. G.; Koridze, A. A. Reactions of iridium bis(phosphinite) pincer complexes with protic acids. *Russ. Chem. Bull.* **2010**, *59*, 745–749.
- (50) Conner, D.; Jayaprakash, K. N.; Cundari, T. R.; Gunnoe, T. B. Synthesis and Reactivity of a Coordinatively Unsaturated Ruthenium-(II) Parent Amido Complex: Studies of X-H Activation (X = H or C). *Organometallics* **2004**, *23*, 2724–2733.
- (51) Connelly, N. G.; Geiger, W. E. Chemical Redox Agents for Organometallic Chemistry. *Chem. Rev.* **1996**, *96*, 877–910.
- (52) Warren, J. J.; Tronic, T. A.; Mayer, J. M. Thermochemistry of Proton-Coupled Electron Transfer Reagents and its Implications. *Chem. Rev.* **2010**, *110*, 6961–7001.
- (53) Mader, E. A.; Manner, V. W.; Markle, T. F.; Wu, A.; Franz, J. A.; Mayer, J. M. Trends in Ground-State Entropies for Transition Metal Based Hydrogen Atom Transfer Reactions. *J. Am. Chem. Soc.* **2009**, *131*, 4335–4345.
- (54) Manner, V. W.; Markle, T. F.; Freudenthal, J. H.; Roth, J. P.; Mayer, J. M. The first crystal structure of a monomeric phenoxy radical: 2,4,6-tri-tert-butylphenoxy radical. *Chem. Commun.* **2008**, 256–258.
- (55) The corresponding free energies were also calculated for the analogue of 2-H lacking methyl groups at the 2- and 6-positions, and for (p-MeO-PCP)IrHCl. For the truncated analogue of 2-H, ΔG_{MLPT} is calculated to be 7.2 kcal/mol, only 0.7 kcal/mol greater than for 2-H. For (p-MeO-PCP)IrHCl, ΔG_{MLPT} is calculated to be 60.7 kcal/mol, the very large value reflecting the electron-donating ability of the methoxy group and its weak basicity. The full data are found in the [Supporting Information](#).
- (56) Morris, R. H. Estimating the Acidity of Transition Metal Hydride and Dihydrogen Complexes by Adding Ligand Acidity Constants. *J. Am. Chem. Soc.* **2014**, *136*, 1948–1959.
- (57) Curtis, C. J.; Miedaner, A.; Ciancanelli, R.; Ellis, W. W.; Noll, B. C.; Rakowski DuBois, M.; DuBois, D. L. [Ni-(Et₂PCH₂NMeCH₂PET₂)₂]⁺ as a Functional Model for Hydrogenases. *Inorg. Chem.* **2003**, *42*, 216–227.
- (58) Brookhart, M.; Green, M. L. H.; Parkin, G. Agostic Interactions in Transition Metal Compounds. *Proc. Natl. Acad. Sci. U. S. A.* **2007**, *104*, 6908–6914.
- (59) The slightly lower (by 0.3 kcal/mol) Gibbs free energy of TS-2[‡]_{benz} relative to 4-H⁺ means, in practice, that the purely kinetic barrier to the reaction is negligible.
- (60) Hebden, T. J.; Schrock, R. R.; Takase, M. K.; Muller, P. Cleavage of dinitrogen to yield a (t-BuPOCOP)molybdenum(IV) nitride. *Chem. Commun.* **2012**, *48*, 1851–1853.
- (61) Leoni, P.; Pasquali, M.; Sommovigo, M.; Laschi, F.; Zanello, P.; Albinati, A.; Lianza, F.; Pregosin, P. S.; Ruegger, H. Chemistry of phosphido-bridged palladium(I) dimers. eta-2-Pd-H-P interactions: a new bonding mode for secondary phosphines. *Organometallics* **1993**, *12*, 1702–1713.
- (62) Albinati, A.; Lianza, F.; Pasquali, M.; Sommovigo, M.; Leoni, P.; Pregosin, P. S.; Ruegger, H. Palladium-hydrogen-phosphorus bridging in a palladium(I) dimer. *Inorg. Chem.* **1991**, *30*, 4690–4692.
- (63) Williams, D. B.; Kaminsky, W.; Mayer, J. M.; Goldberg, K. I. Reactions of iridium hydride pincer complexes with dioxygen: new dioxygen complexes and reversible O₂ binding. *Chem. Commun.* **2008**, 4195–4197.
- (64) Alvarez, E.; Conejero, S.; Paneque, M.; Petronilho, A.; Poveda, M. L.; Serrano, O.; Carmona, E. Iridium(III)-Induced Isomerization of 2-Substituted Pyridines to N-Heterocyclic Carbenes. *J. Am. Chem. Soc.* **2006**, *128*, 13060–13061.

(65) Álvarez, E.; Conejero, S.; Lara, P.; López, J. A.; Paneque, M.; Petronilho, A.; Poveda, M. L.; del Río, D.; Serrano, O.; Carmona, E. Rearrangement of Pyridine to Its 2-Carbene Tautomer Mediated by Iridium. *J. Am. Chem. Soc.* **2007**, *129*, 14130–14131.

(66) Mohammad, H. A. Y.; Grimm, J. C.; Eichele, K.; Mack, H.-G.; Speiser, B.; Novak, F.; Kaska, W. C.; Mayer, H. A. Double cyclometalation: Implications for C-H oxidative addition with PCP pincer compounds of iridium. *ACS Symp. Ser.* **2004**, *885*, 234–247.

(67) Novak, F.; Speiser, B.; Mohammad, H. A. Y.; Mayer, H. A. Electrochemistry of transition metal complex catalysts: Part 10. Intra- and intermolecular electrochemically activated C-H addition to the central metal atom of a P–C–P-pincer iridium complex. *Electrochim. Acta* **2004**, *49*, 3841–3853.

(68) Das, K.; Kumar, A. Alkane dehydrogenation reactions catalyzed by pincer-metal complexes. *Adv. Organomet. Chem.* **2019**, *72*, 1–57.

(69) Kumar, A.; Bhatti, T. M.; Goldman, A. S. Dehydrogenation of Alkanes and Aliphatic Groups by Pincer-Ligated Metal Complexes. *Chem. Rev.* **2017**, *117*, 12357–12384.

(70) Fang, H.; Liu, G.; Huang, Z. In *Pincer Compounds Chemistry and Applications*; Morales-Morales, D., Ed.; Elsevier B.V.: Amsterdam, 2018; pp 383–399.

(71) Gordon, B. M.; Lease, N.; Emge, T. J.; Hasanayn, F.; Goldman, A. S. Reactivity of Iridium Complexes of a Triphosphorus-Pincer Ligand Based on a Secondary Phosphine. Catalytic Alkane Dehydrogenation and the Origin of Extremely High Activity. *J. Am. Chem. Soc.* **2022**, *144*, 4133–4146.

(72) Reamey, R. H.; Whitesides, G. M. Mechanism of hydrogenolysis of dineopentylbis(triethylphosphine)platinum(II). *J. Am. Chem. Soc.* **1984**, *106*, 81–85.

(73) Jones, W. D.; Feher, F. J. Kinetics and thermodynamics of intra- and intermolecular carbon-hydrogen bond activation. *J. Am. Chem. Soc.* **1985**, *107*, 620–631.

(74) To capture the low entropic penalty associated with the addition of an alkane molecule in alkane solvent or at a very high concentration of alkane, the reaction was calculated with a van der Waals complex of the metal complex and an alkane molecule as reactant, rather than free metal complex and a gas-phase alkane molecule. See ref 75.

(75) Zhou, X.; Malakar, S.; Dugan, T.; Wang, K.; Sattler, A.; Marler, D. O.; Emge, T. J.; Krogh-Jespersen, K.; Goldman, A. S. Alkane Dehydrogenation Catalyzed by a Fluorinated Phebox Iridium Complex. *ACS Catal.* **2021**, *11*, 14194–14209.

(76) Smidt, J.; Hafner, W.; Jira, R.; Sedlmeier, J.; Sieber, R.; Rüttinger, R.; Kojer, H. Katalytische Umsetzungen von Olefinen an Platinmetall-Verbindungen Das Consortium-Verfahren zur Herstellung von Acetaldehyd. *Angew. Chem.* **1959**, *71*, 176–182.

(77) Shada, A. D. R.; Miller, A. J. M.; Emge, T. J.; Goldman, A. S. Catalytic Dehydrogenation of Alkanes by PCP–Pincer Iridium Complexes Using Proton and Electron Acceptors. *ACS Catal.* **2021**, *11*, 3009–3016.